

m6A RNA methylation regulators were associated with the malignancy and prognosis of ovarian cancer

Liu jinhui

The first affiliated hospital of nanjing medical university

Li siyue

The first affiliated hospital of nanjing medical university

Nie sipei

The first affiliated hospital of nanjing medical university

Shen yujie

The first affiliated hospital of nanjing medical university

Meng huangyang

The first affiliated hospital of nanjing medical university

Sun rui

The first affiliated hospital of nanjing medical university

Yang jing

The first affiliated hospital of nanjing medical university

Wenjun Cheng (✉ wenjunchengdoc@163.com)

Jiangsu Province Hospital and Nanjing Medical University First Affiliated Hospital

<https://orcid.org/0000-0002-3872-4384>

Research

Keywords: Ovarian cancer, m6A, prognosis, immune cells infiltration, TCGA

Posted Date: April 23rd, 2020

DOI: <https://doi.org/10.21203/rs.3.rs-23755/v1>

License: © ⓘ This work is licensed under a Creative Commons Attribution 4.0 International License.

[Read Full License](#)

Abstract

M6A is a process of RNA methylation. Ovarian cancer poses a great threat to women's life. Abnormal modification of RNA may play a regulatory role in tumor development. RNA and clinical information come from GTEx and TCGA. "limma" was used for pre-analysis. "ConsensusClusterPlus" was used to group samples. Enrich Database was introduced for functional analysis. PPI complex was generated in STRING. GSEA was conducted to explore associated pathways. Regression model was constructed to screen hub genes. cBioPortal tool was used to compare the genetic alterations. TIMER database was used to analyze the abundance of tumor-infiltrating immune cells. "rms" package was used for nomogram and calibrate curve. Kaplan-Meier curve analysis was conducted to compare the survival time. ROC curve analysis was performed to estimate the predictive value of related genes. We analyzed the association between each m6A RNA methylation regulator and the clinical features of OC. Survival analysis showed that ALKBH5, METTL14, METTL16, YTHDF1, YTHDF2, YTHDF3 and ZC3H13 were significantly associated. We further found that METTL3 was central gene in the network of m6A RNA methylation regulators. Its interactions or co-expressions with KIAA1429, METTL14, WTAP, YTHDF1, YTHDF3, YTHDF2 and YTHDC1 were confirmed in the String database. METTL3 was also significantly correlated with YTHDC2 and YTHDF3. The expression profiles of METTL3, YTHDC2 and YTHDF3 were all related to the clinicopathological features in OC. GSEA identified pathways involved in graft versus host disease and oxidative phosphorylation. Regression models identified prognosis-associated HNRNPA2B1, KIAA1429 and WTAP. Dendritic fraction, macrophage fraction and neutrophil fraction were associated with three m6A regulators. YTHDF1, WTAP and ZC3H13 showed the most diverse alterations. Our study analyzed the association between m6A regulators and clinical features of OC. HNRNPA2B1, KIAA1429 and WTAP showed high prognostic value and they participate in OC through regulating the dendritic fraction, macrophage fraction and neutrophil fraction of immune cells. This research provides a new direction for the future research on OC.

Background

Epigenetic modification is a change in the expression of a nucleotide sequence. Previous studies have shed light on the epigenetic pathways such as histone modification, chromosome remodeling, DNA methylation, non-coding RNA regulation. RNA-level modification can be accomplished by N7-methyladenosine, N1-methyladenosine, pseudouridine, 5-methylcytosine, N6, 2'-O-methylation and 2'-O-dimethyladenosine (m6A). Among them, m6A is a form of RNA methylation discovered in the 1970s.

RNA methylation, like DNA methylation, is a dynamic and reversible process involving methyltransferases "writers", binding proteins ("readers"), and demethylases ("erasers"). The prominent m6A methylation regulators included "writers" like METTL3, METTL14, WTAP, KIAA1429, RBM15 and ZC3H13; "readers" like YTHDC1, YTHDC2, YTHDF1, YTHDF2 and HNRNPC; "erasers" like FTO and ALKBH5. More and more studies have found that regulators in m6A RNA methylation are associated with tumorigenesis. For example, Chen M et al. found that METTL3 promoted liver cancer progression¹. Li J et al. found that

FTO promoted the growth of lung cancer cells by regulating the m6A level of USP7 mRNA². Hua W et al. found that METTL3 promoted ovarian carcinoma growth and invasion³

Ovarian cancer poses a great threat to women's life. Abnormal modification of RNA may act in tumor development. This study systematically analyzed the relationship between m6A RNA methylation regulators and the clinical features of ovarian cancer, providing a new direction for future research on ovarian carcinogenesis.

Materials And Methods

Data Sources

The RNA-seq data and corresponding clinicopathological data were obtained from TCGA (<http://cancergenome.nih.gov/>) including 379 OC patients⁴. In order to analysis the different between normal ovarian tissues and ovarian cancer ,the expression dataset (N = 379 for ovarian cancer from TCGA and N = 88 for normal ovarian tissues from GTEx) were downloaded from the UCSC Xena project (<http://xena.ucsc.edu/>) .we renormalized data based on total reads for each sample to generate RPKM (Reads Per Kilobase of transcript per Million mapped reads)⁵ and then compare the expression of between normal ovarian and OC tissues. “limma” package⁶ was performed to solve the imbalance between the tumor and normal data and then analyze the different expression among normal ovarian and OC

Selection of m6A RNA methylation regulators

We have identified 17 m6A RNA methylation regulators from published papers for follow-up studies.

Bioinformatic analysis

To investigate the function of m6A RNA methylation regulators in OC, we divided samples into different groups using “ConsensusClusterPlus”⁷. In order to functionally annotate genes that are differentially expressed in different groups, Enrich Database (<https://amp.pharm.mssm.edu/Enrichr/>)⁸ was conducted for functional analysis. Interactions among m6A RNA methylation regulators were analyzed using the STRING database (<http://www.string-db.org/>)⁹. Gene Set Enrichment Analyses (GSEA)¹⁰ was for identifying the functions based on different subgroups of OC. Univariate Cox regression analyses was used to determine the prognostic value of m6A RNA methylation regulators. From this, we identified 3 genes significantly associated with survival ($P < 0.05$), which we selected for further functional analysis and development of a potential risk signature with the LASSO Cox regression algorithm. The minimum criteria was set to determine the 3 genes and their coefficients. The risk score for the signature was calculated using the formula: Risk score = $\sum \text{Coef}_i * x_{ini} = 1$, where Coef_i is the coefficient, and x_i is the z-

score-transformed relative expression value of each selected gene. This formula was used to calculate a risk score for each patient in TCGA datasets. To reveal potential underlying Kyoto Encyclopedia of Genes and Genomes (KEGG) pathways of the high - and low - risk groups and 3 prognosis-related genes, GSEA were utilized to find enriched terms in C2 in TCGA-OV database. $p < 0.05$ were considered statistically significant.

cBioPortal database (<http://www.cbioportal.org/>)¹¹ is an open access tool which provides analysis, visualization and downloads of cancer genomics datasets of many types of tumors. Complex cancer genomics profiles are accessible from the cBioPortal tool, thus enabling us to compare the genetic alterations of the three genes based on prognosis signature in ovarian cancer.

The abundances 6 subtypes of tumor-infiltrating immune cells including CD4 T cells, CD8 T cells, B cells, neutrophils, macrophages and dendritic cells can be visualized by TIMER online database¹².

Construction and validation of the nomogram

A nomogram and calibrate curve was constructed using the “rms” package on R. To quantify the discrimination performance of this nomogram, Harrel’s concordance index (C-index) was measured. The nomogram was then subjected to bootstrapping validation (1,000 bootstrap resamples) to calculate a relatively corrected C-index¹³. Finally, we used decision curve analysis (DCA) to determine the clinical usefulness of the nomogram¹⁴.

Statistical analysis

Patients were divided into two clusters by consensus expression of m6A RNA methylation regulators. Chi-square tests were used to compare the distribution of grade, race, stage age and tumor status between the two risk groups.

Patients were then divided into two groups based on the median levels of risk score. This prognostic model and patient survival information were merged. Kaplan-Meier survival curves were used to compare the prognostic ability of prediction models. Area under the curve (AUC) value for the ROC curves of each prognostic model was calculated by survival.ROC package in R. Besides, univariate and multivariate Cox regression analysis were conducted to compare the hazard ratio (HRs) of prognostic models and important clinical features for OC. Differences among clinical parameters(age, grade, stage and tumor-status)were tested using independent t-tests and $P < 0.05$ were considered to be statistically significant.

Results

Expression of m6A RNA methylation regulators was correlated with OC clinicopathological features

We analyzed the correlation between each m6A RNA methylation regulator and OC clinical features. These clinical features include age, grade, stage, and tumor-status. FMR1, METTL16, RBM15 and WTAP had significant correlation with age (**Supporting Fig. 1**). FTO and YTHDC2 had significant correlation with OC grade (**Supporting Fig. 2**). ALKBH5, METTL3, METTL14, METTL16, RBM15 and YTHDF1 had significant correlation with OC stage (**Supporting Fig. 3**). HNRNPA2B1 and METTL16 had significant correlation with OC status (**Supporting Fig. 4**). For ovarian cancer, BRCA1 gene mutation is a common pathogenic factor and marker for ovarian cancer¹⁵. We also analyzed the expression of the m6A RNA methylation regulator in ovarian cancer patients with and without BRCA1 mutation, finding that expression of both FMR1 and YTHDF1 showed difference between BRCA1-mutation and non-BRCA1-mutation groups (**Supporting Fig. 5**). We analyzed 17 m6A RNA methylation regulators in OC tissue samples and normal tissue samples, finding that all the regulators were differentially expressed (Fig. 1). In addition, survival analysis found that the overall survival (OS) and progression-free survival (PFS) of ALKBH5, METTL14, METTL16, YTHDF1, YTHDF2, YTHDF3 and ZC3H13 were meaningful (**Supporting Fig. 6 and Supporting Fig. 7**). To assess the diagnostic value of 17 m6A RNA regulators, we generated a ROC curve using the expression data from ovarian cancer patients and healthy (**Supporting Fig. 8**). The area under the ROC curve (AUC) indicated a modest diagnostic value.

Two clusters of m6A RNA methylation regulators were associated with distinct OC clinical outcomes and clinicopathological features

With clustering stability increasing from $k = 2$ to 10, $k = 2$ seemed to be an adequate selection based on the expression similarity of m6A RNA methylation regulators. (Fig. 2A-C). Then, 379 OC samples were clustered into two subgroups in the TCGA dataset (cluster1:216; cluster2:163). We named the 2 subgroups to be cluster1 and cluster2 and compared clinicopathological features of the 2 two clusters by $k = 2$ (Fig. 2D). A significantly shorter OS was displayed in Cluster 1 than in Cluster 2 (Fig. 2E).

Categories identified by consensus clustering are closely associated with the progression of OC

In order to understand the interactions among the seventeen m6A RNA methylation regulators, We analyzed the interaction (Fig. 3A) and correlation (Fig. 3B) among these regulators. METTL3 lay at the core of the network of m6A RNA methylation regulators. Its interactions or co-expressions with KIAA1429, METTL14, WTAP, YTHDF1, YTHDF3, YTHDF2 and YTHDC1 were constructed and displayed in the String database. METTL3 was also significantly correlated with the YTHDC2 and YTHDF3. Three genes might co-work to regulate the progression of OC. We further performed the functional analysis of the 2 clusters. GSEA was functioned to show that the most relative GO term were chemokine activity, macrophage chemotaxis, macrophage migration, monocyte chemotaxis and tumor necrosis factor biosynthetic

process in cluster 1 and cluster 2. (Fig. 3C). The most relative pathway were allograft rejection, asthma, graft versus host disease, oxidative phosphorylation and ribosome (Fig. 4). Above findings suggested that the 2 categories identified by consensus clustering are closely associated with the progression of OC.

m6A RNA methylation regulators had prognostic significance

We investigated the prognostic ability of m6A RNA methylation regulators in OC. Univariate Cox regression analysis was conducted according to the expression levels of m6A RNA methylation regulators ((Fig. 5A). The results indicated that three genes were significantly correlated with OS ($P < 0.05$). WTAP and KIAA1429 were two risky genes with $HR > 1$, while HNRNPA2B1 was a risky gene with $HR < 1$.

To evaluate the ability of m6A RNA methylation regulators in predicting the clinical outcomes of OC, we performed LASSO Cox regression algorithm on the three prognosis-associated genes (Fig. 5B-C), which were selected to construct the risk signature based on the minimum criteria. Coefficients obtained from LASSO algorithm were used to calculate the risk score: $HNRNPA2B1 * -0.01 + KIAA1429 * 0.085 + WTAP * 0.03$. We separated the OC samples ($n = 374$) into low-and high-risk groups based on the median risk score. The distribution of risk score, survival status, and the expression of three genes from each patient were also displayed (Fig. 5D-F). Significant difference was observed in OS between the two groups (Fig. 6A). ROC curves for 5-year survival were used to reveal the predictive performance of the three genes risk signature. The 5-year AUC of the signature was 0.649, which was obviously higher than that of stage (AUC = 0.512), grade (AUC = 0.525) and age (AUC = 0.539) (Fig. 6B). The results showed the three-gene risk signature had a stronger ability to predict OC survival than clinical factors.,

Prognostic value and clinical utility of three m6A regulators

Based on TCGA dataset, we constructed univariate and multivariate regression models to identify whether the risk signature was an independent prognostic factor. Univariate analysis showed that tumor status and risk score were both correlated with OS (Fig. 6C). Having absorbed three genes into the multivariate regression analysis, tumor status and risk score remained significantly correlated with the OS (Fig. 6D). We also explored the clinical features associated with the three genes and Risk score (Table 1). We found that WTAP expression level was significantly different in different age groups (Fig. 6E). The expression levels of HNRNPA2B1 in the TUMOR FREE group and the TUMOR group were also significantly different (Fig. 6F). Risk score of patients in different age groups were also significantly different (Fig. 6G). Then, the stratification analysis was performed based on grade, age, stage and tumor status. Patients were stratified into Grade I/II and Grade III/IV subgroups, Stage I/II and Stage III/IV subgroups. As shown in **Supporting Fig. 9A**, the prognosis of high risk patients was significantly worse than that of low risk patients in the Stage III/IV subgroup, which was consistent with the results of Grade

II/IV subgroup (**Supporting Fig. 9B**). However, there was no statistical significance in Stage I/II subgroup and Grade I/II subgroup. We also assessed the prognostic ability of the three-gene signature combined with age and tumor status. The patients were also stratified into different subgroups, ≥ 60 years subgroup and < 60 years subgroup. Interestingly, we found that high risk patients in two subgroups were inclined to unfavorable OS (**Supporting Fig. 9C-E**). Most of the immunity-related pathways, like T cell receptor signaling pathway, cytokine cytokine receptor interaction and TOLL like receptor signaling pathway, were enriched in the high risk group, whereas most of the immunity-unrelated pathways, like DNA replication and linoleic acid metabolism, were enriched in the low risk group (Fig. 7A). The three genes from the risk score model were co-enriched in cell adhesion molecules cams and chemokine signaling pathway (Fig. 7B).

Table 1
Clinical significance of 3 prognosis-related genes.

Gene	Age		Stage		Grade		Tumor Status	
	(≥ 60 / <60)		(I-II/III-IV)		(1-2/3-4)		(with tumor/tumor free)	
	T	P	T	P	T	P	T	P
HNRNPA2B1	-0.165	0.869	1.49	0.154	-0.571	0.570	2.844	0.005
KIAA1429	-0.615	0.539	1.909	0.072	-1.268	0.209	0.082	0.935
WTAP	3.641	3.264e-04	1.337	0.198	1.218	0.230	-0.146	0.884

Bold values indicate $P < 0.05$.

Association between three m6A regulators and immune infiltration

We used TCGA dataset to search the most significant tumor-infiltrating immune cells. Risk score was calculated to indicate the association between immune infiltration and three m6A regulators. Interestingly, we found that Dendritic fraction, Macrophage fraction and Neutrophil fraction were mostly enriched in high risk group (**Supporting Fig. 7A-C**).

A nomogram based on three m6A regulators

Encompassing age, stage, grade, tumor status and risk score, a nomogram was constructed to predict the three- or five-year OS of OC (Fig. 8A). The calibration curve from Fig. 8B-C suggested that the nomogram exhibited a performance as good as that of the Kaplan–Meier estimates. The C-index for this nomogram was 0.789 and became 0.773 after bootstrapping validation, suggestive of its good discriminating ability. Meanwhile, DCA was created to estimate the clinical utility of the nomogram. The result of DCA showed

that the nomogram containing three mRNAs" signature had better prediction ability with a threshold ranging from 2 to 83% (Fig. 8D).

Genetic information of the seventeen genes

The genetic alteration harbored in the seventeen genes was analyzed with cBioPortal software. The network constructed by METTL3, HNRNPA2B1, HNRNPC, FMR1 and their 50 most associated neighbor genes were exhibited (only four out of the seventeen genes had a joint node, while the remaining three genes had no junctions and were not shown) (**Supporting Fig. 11A**). **Supporting Fig. 11B-C** illustrated that the seventeen genes were altered in 471 (79%) of the 594 cases/patients (606 in total); YTHDF1, WTAP and ZC3H13 showed the most diverse alterations, including amplification, missense mutation etc.

Discussion

Ovarian cancer is the most common gynecological malignancy. Most of the women have developed advanced stage when diagnosed¹⁶. Early diagnosis is critical to improve OC prognosis, because a local stage has a 5-year relative survival rate of 93%. Specific biological diagnostic markers have been defined¹⁷. m6A modification has been implicated in mRNA turnover, localization or translation^{18,19,20}. METTL3 has shown a role in ovarian cancer³. Therefore, we reasonably speculate that m6A RNA methylation regulators are associated with ovarian cancer. We identified two OC subgroups (Cluster1 and Cluster 2) based on the expression of m6A RNA methylation regulators. Two clusters were not only associated with OC prognosis and clinicopathological features, but e also some functional pathways, including graft versus host disease and oxidative phosphorylation. Coincidentally, these functional pathways have been found to regulate the development of OC. For example, Bay JO et al. found that an OC patient developed acute graft-versus-host disease and from this time her tumor diminished progressively²¹. Hänel M et al. also discovered a graft-versus-tumor²² effect in refractory ovarian cancer. Pastò A et al. found oxidative phosphorylation in the stem cells from epithelial ovarian cancer patients²³. Oxidative phosphorylation has been also validated as a therapeutic target for ovarian cancer²⁴.

METTL3 is the most widely studied writer. The experiments of Hua W et al. demonstrated that METTL3 promoted ovarian carcinoma growth and invasion through regulating AXL translation and epithelial to mesenchymal transition³. Cai X et al. demonstrated that HBXIP-elevated METTL3 expression promoted the progression of breast cancer via inhibiting tumor suppressor let-7g²⁵. Vu LP et al. found that METTL3 curbed myeloid differentiation of normal hematopoietic and leukemia cells²⁶. METTL3 influences the progression of renal cell carcinoma and pancreatic cancer^{27,28}. We identified METTLE3, as the central gene in the network of m6A RNA methylation regulators, co-worked with the others in OC development. This conclusion has been proven in previous studies²⁹

Another writer associated with ovarian cancer is WTAP³⁰. Consistently, our results showed that WTAP had a mutation rate of 16% and was highly expressed in patients aged over 60. The older age, the greater

cumulative mutational load. The prognosis of bladder cancer and malignant glioma are also affected by WTAP^{31,32}.

METTL14 is the main factor involved in aberrant m6A modification. Ma JZ et al. found that METTL14 as a writer suppressed the metastatic potential of hepatocellular carcinoma by modulating N6-methyladenosine-dependent primary microRNA processing³³. In our study, METTL14 was lowly expressed in ovarian cancer samples, highly expressed in patients of Stage 1/2 subgroup and correlated with OC prognosis, thus we can see that the same M6A regulator also exerted different effects in different tumors.

KIAA1429, METTL16, RBM15 and ZC3H13 were less studied in tumors. Qian JY et al. found that KIAA1429 acted as an oncogenic factor in breast cancer by regulating CDK1 in an N6-methyladenosine-independent manner³⁴. KIAA1429 also been proved to participate in the migration and invasion of hepatocellular carcinoma³⁵. ZC3H13 was found to suppress colorectal cancer proliferation and invasion³⁶. We found that ZC3H13 showed a mutation rate of 18% and highly expressed in OC samples, and its expression level was negatively correlated with OC prognosis. Our results showed that METTL16 was lowly expressed in OC tissues and was positively correlated with the prognosis. METTL16 was lowly expressed in the samples collected from patients younger than 60, The same trend were shown in patients of stage III-IV subgroup and with tumor subgroup. These results supported our hypothesis that METTL16 suppressed the development of OC. These findings indicated that increasing the level of m6A enrichment which was conducted by writer can indeed alter the development of the tumor. However, the specific mechanism still needs to be tapped.

As complementary factors of writers, erasers also exert effects on a variety of tumors. Obesity is a high risk factor for many tumors³⁷, and fat mass and obesity (FTO) is associated with obesity³⁸. Akbari ME et al. found that FTO gene affected obesity and breast cancer through similar mechanisms³⁹. FTO is associated with the occurrence and prognosis of gastric cancer⁴⁰. Alkylation repair homolog protein 5 (ALKBH5) is also associated with pancreatic cancer⁴¹, gastric cancer⁴² and breast cancer⁴³. Zhu H et al. found that ALKBH5 inhibited autophagy of epithelial ovarian cancer through regulating miR-7 and BCL-2⁴⁴.

Three readers (YTHDF1, YTHDF2 and YTHDF3) were all highly expressed in OC samples and negatively related with prognosis. YTHDF1, YTHDF2 and HNRNPC have been intensely studied. YTH domain family 1 (YTHDF1) has a mutation rate of 27% and high expression in OC samples, which is associated with the poor prognosis of OS and DFS. YTHDF1 has been shown to be involved in the regulation of colorectal and pancreatic cancer^{45,46}. Overexpression of YTHDF1 is associated with the poor prognosis of hepatocellular carcinoma⁴⁷. In pancreatic cancer cells, YTHDF2 orchestrates epithelial-mesenchymal transition/proliferation dichotomy⁴⁶. Li J et al. found that downregulation of N6-methyladenosine binding YTHDF2 protein mediated by miR-493-3p suppressed prostate cancer⁴⁸. YTHDF2 has also a certain regulatory effect in lung cancer and gastric cancer^{49,50}. HNRNPC can serve as a candidate biomarker for

chemoresistance in gastric cancer⁵¹. Interestingly, Kleemann M et al. demonstrated that MiR-744-5p could induce cell death by directly targeting HNRNPC and NFIX in ovarian cancer⁵². The BRCA gene mutation is a feature of hereditary ovarian cancer. We classified the samples according to the presence of BRCA gene mutation⁵³, finding that the expression of FMR1 was related to BRCA gene mutation. Gleicher N et al. also found that BRCA/FMR1 had correlation with ovarian cancer⁵⁴. The mechanism through which BRCA/FMR1 mutation leads to ovarian cancer is worthy of further investigation.

Our prognostic regression analysis found that HNRNPA2B1, KIAA1429 and WTAP have the strongest correlation with OC. Subsequently, we stratified OC patients into two subgroups with statistically different survival outcomes. Besides, univariate and multivariate Cox analyses identified the prognostic signature as an independent factor. In the present study, owing to the lack of external validation cohort, we could not validate the prognostic performance of the 3-mRNA signature. Thus, we applied bootstrapping with 1,000 resample to internally validate the performance of 3-mRNA signature. The C-index for the internal validation was 0.773, indicating its good performance in clinical use. Moreover, we built a nomogram containing the 3-mRNA signature and other clinical features of ovarian cancer. The nomogram showed a moderate performance in predicting the survival of OC patients. Meanwhile, the result of DCA suggested that the nomogram showed better prediction ability with a threshold ranging from 2–83%. Except WTAP, the role of both HNRNPA2B1 and KIAA1429 in ovarian cancer has not been thoroughly studied and can be used to direct further research. GSEA showed that the samples from the high-risk group were mainly enriched in immune-related pathways. Interestingly, we further identified that the Dendritic fraction, Macrophage fraction and Neutrophil fraction were related to the three m6A regulators. Surprisingly, there are experiments demonstrating that dendritic cell (DC) immunotherapy can induce anti-tumor T cell immunity⁵⁵. Macrophage can regulate the progress of OC through multiple mechanisms like CD47⁵⁶ and NF- κ B activation⁵⁷. Meta-analysis by Chen S et al. shows neutrophil-to-lymphocyte ratio is a potential prognostic biomarker in patients with ovarian cancer⁵⁸. It can be seen that distorted immune microenvironment may induce tumors to some extent.

Our research has the following shortcomings: 1. The model is not validated with external data. 2. Lack of verification of in vitro and in vivo experiments. Prospective clinical trials are necessary in the future to reconfirm our findings.

Conclusion

Our study analyzed the association between m6A regulators and clinical features of OC. HNRNPA2B1, KIAA1429 and WTAP showed high prognostic value for OC and they participate in the process of ovarian cancer through regulating the dendritic fraction, macrophage fraction and neutrophil fraction of immune cells. This research provides a new direction for the future research on ovarian cancer.

Abbreviations

Ovarian cancer (OC)

protein–protein interaction (PPI)

Search Tool for the Retrieval of Interacting Genes Database (STRING)

Molecular Complex Detection (MCODE)

Receiver operating characteristic (ROC)

Gene set enrichment analysis (GSEA)

Decision curve analysis (DCA)

Kyoto Encyclopedia of Genes and Genomes (KEGG)

Area under the curve (AUC)

Hazard ratio (HR)

Declarations

Author contribution

Authors Wenjun Cheng and Jinhui Liu designed the project. Authors Jinhui Liu, SiYue Li and Sipei Nie contributed on data analysis and prepared the main manuscript. All authors reviewed the manuscript.

Acknowledgements

Not applicable.

Funding

This work was supported by the National Nature Science Foundation of China (81872119) and Jiangsu province medical innovation team (CXTDA2017008).

Competing interests statement

The authors declare that they have no competing interests.

Data availability statement

The data and materials can be found from the first author and corresponding author.

Ethics approval and consent to participate

Not applicable.

Consent for publication

Written informed consent for publication was obtained from all participants.

References

1. Chen M, *et al.* RNA N6-methyladenosine methyltransferase-like 3 promotes liver cancer progression through YTHDF2-dependent posttranscriptional silencing of SOCS2. *Hepatology (Baltimore, Md)* **67**, 2254-2270 (2018).
2. Li J, *et al.* The m6A demethylase FTO promotes the growth of lung cancer cells by regulating the m6A level of USP7 mRNA. *Biochem Biophys Res Commun* **512**, 479-485 (2019).
3. Hua W, *et al.* METTL3 promotes ovarian carcinoma growth and invasion through the regulation of AXL translation and epithelial to mesenchymal transition. *Gynecologic oncology* **151**, 356-365 (2018).
4. Tomczak K, Czerwinska P, Wiznerowicz M. The Cancer Genome Atlas (TCGA): an immeasurable source of knowledge. *Contemporary oncology (Poznan, Poland)* **19**, A68-77 (2015).
5. Wagner GP, Kin K, Lynch VJ. Measurement of mRNA abundance using RNA-seq data: RPKM measure is inconsistent among samples. *Theory in biosciences = Theorie in den Biowissenschaften* **131**, 281-285 (2012).
6. Ritchie ME, *et al.* limma powers differential expression analyses for RNA-sequencing and microarray studies. *Nucleic acids research* **43**, e47 (2015).
7. Wilkerson MD, Hayes DN. ConsensusClusterPlus: a class discovery tool with confidence assessments and item tracking. *Bioinformatics (Oxford, England)* **26**, 1572-1573 (2010).
8. Keenan AB, *et al.* ChEA3: transcription factor enrichment analysis by orthogonal omics integration. *Nucleic acids research* **47**, W212-w224 (2019).
9. von Mering C, Huynen M, Jaeggi D, Schmidt S, Bork P, Snel B. STRING: a database of predicted functional associations between proteins. *Nucleic acids research* **31**, 258-261 (2003).
10. Subramanian A, Kuehn H, Gould J, Tamayo P, Mesirov JP. GSEA-P: a desktop application for Gene Set Enrichment Analysis. *Bioinformatics (Oxford, England)* **23**, 3251-3253 (2007).
11. Gao J, *et al.* Integrative analysis of complex cancer genomics and clinical profiles using the cBioPortal. *Science signaling* **6**, pl1 (2013).
12. Li T, *et al.* TIMER: A Web Server for Comprehensive Analysis of Tumor-Infiltrating Immune Cells. *Cancer research* **77**, e108-e110 (2017).

13. Pencina MJ, D'Agostino RB. Overall C as a measure of discrimination in survival analysis: model specific population value and confidence interval estimation. *Statistics in medicine* **23**, 2109-2123 (2004).
14. Vickers AJ, Elkin EB. Decision curve analysis: a novel method for evaluating prediction models. *Medical decision making : an international journal of the Society for Medical Decision Making* **26**, 565-574 (2006).
15. Liu WL, *et al.* [Association between single nucleotide polymorphism of BARD1 gene and BRCA1 gene mutation in epithelial ovarian cancer]. *Zhonghua fu chan ke za zhi* **52**, 403-410 (2017).
16. Torre LA, *et al.* Ovarian cancer statistics, 2018. *CA: a cancer journal for clinicians* **68**, 284-296 (2018).
17. Scaletta G, *et al.* The role of novel biomarker HE4 in the diagnosis, prognosis and follow-up of ovarian cancer: a systematic review. *Expert review of anticancer therapy* **17**, 827-839 (2017).
18. Xiao W, *et al.* Nuclear m(6)A Reader YTHDC1 Regulates mRNA Splicing. *Molecular cell* **61**, 507-519 (2016).
19. Fustin JM, *et al.* RNA-methylation-dependent RNA processing controls the speed of the circadian clock. *Cell* **155**, 793-806 (2013).
20. Wang X, *et al.* N(6)-methyladenosine Modulates Messenger RNA Translation Efficiency. *Cell* **161**, 1388-1399 (2015).
21. Bay JO, *et al.* Potential allogeneic graft-versus-tumor effect in a patient with ovarian cancer. *Bone marrow transplantation* **25**, 681-682 (2000).
22. Hanel M, Bornhauser M, Muller J, Thiede C, Ehninger G, Kroschinsky F. Evidence for a graft-versus-tumor effect in refractory ovarian cancer. *Journal of cancer research and clinical oncology* **129**, 12-16 (2003).
23. Pasto A, *et al.* Cancer stem cells from epithelial ovarian cancer patients privilege oxidative phosphorylation, and resist glucose deprivation. *Oncotarget* **5**, 4305-4319 (2014).
24. Nayak AP, Kapur A, Barroilhet L, Patankar MS. Oxidative Phosphorylation: A Target for Novel Therapeutic Strategies Against Ovarian Cancer. *Cancers* **10**, (2018).
25. Cai X, *et al.* HBXIP-elevated methyltransferase METTL3 promotes the progression of breast cancer via inhibiting tumor suppressor let-7g. *Cancer letters* **415**, 11-19 (2018).
26. Vu LP, *et al.* The N(6)-methyladenosine (m(6)A)-forming enzyme METTL3 controls myeloid differentiation of normal hematopoietic and leukemia cells. *Nature medicine* **23**, 1369-1376 (2017).

27. Li X, *et al.* The M6A methyltransferase METTL3: acting as a tumor suppressor in renal cell carcinoma. *Oncotarget* **8**, 96103-96116 (2017).
28. Taketo K, *et al.* The epitranscriptome m6A writer METTL3 promotes chemo- and radioresistance in pancreatic cancer cells. *International journal of oncology* **52**, 621-629 (2018).
29. Scholler E, *et al.* Interactions, localization, and phosphorylation of the m(6)A generating METTL3-METTL14-WTAP complex. *RNA (New York, NY)* **24**, 499-512 (2018).
30. Yu HL, Ma XD, Tong JF, Li JQ, Guan XJ, Yang JH. WTAP is a prognostic marker of high-grade serous ovarian cancer and regulates the progression of ovarian cancer cells. *OncoTargets and therapy* **12**, 6191-6201 (2019).
31. Chen L, Wang X. Relationship between the genetic expression of WTAP and bladder cancer and patient prognosis. *Oncol Lett* **16**, 6966-6970 (2018).
32. Xi Z, Xue Y, Zheng J, Liu X, Ma J, Liu Y. WTAP Expression Predicts Poor Prognosis in Malignant Glioma Patients. *Journal of molecular neuroscience : MN* **60**, 131-136 (2016).
33. Ma JZ, *et al.* METTL14 suppresses the metastatic potential of hepatocellular carcinoma by modulating N(6) -methyladenosine-dependent primary MicroRNA processing. *Hepatology (Baltimore, Md)* **65**, 529-543 (2017).
34. Qian JY, *et al.* KIAA1429 acts as an oncogenic factor in breast cancer by regulating CDK1 in an N6-methyladenosine-independent manner. *Oncogene* **38**, 6123-6141 (2019).
35. Cheng X, *et al.* KIAA1429 regulates the migration and invasion of hepatocellular carcinoma by altering m6A modification of ID2 mRNA. *OncoTargets and therapy* **12**, 3421-3428 (2019).
36. Zhu D, *et al.* ZC3H13 suppresses colorectal cancer proliferation and invasion via inactivating Ras-ERK signaling. *Journal of cellular physiology* **234**, 8899-8907 (2019).
37. Deng X, Su R, Stanford S, Chen J. Critical Enzymatic Functions of FTO in Obesity and Cancer. *Frontiers in endocrinology* **9**, 396 (2018).
38. Zhao X, Yang Y, Sun BF, Zhao YL, Yang YG. FTO and obesity: mechanisms of association. *Current diabetes reports* **14**, 486 (2014).
39. Akbari ME, Gholamalizadeh M, Doaei S, Mirsafa F. FTO Gene Affects Obesity and Breast Cancer Through Similar Mechanisms: A New Insight into the Molecular Therapeutic Targets. *Nutrition and cancer* **70**, 30-36 (2018).
40. Xu D, Shao W, Jiang Y, Wang X, Liu Y, Liu X. FTO expression is associated with the occurrence of gastric cancer and prognosis. *Oncology reports* **38**, 2285-2292 (2017).

41. Cho SH, *et al.* ALKBH5 gene is a novel biomarker that predicts the prognosis of pancreatic cancer: A retrospective multicohort study. *Annals of hepato-biliary-pancreatic surgery* **22**, 305-309 (2018).
42. Zhang J, *et al.* ALKBH5 promotes invasion and metastasis of gastric cancer by decreasing methylation of the lncRNA NEAT1. *Journal of physiology and biochemistry* **75**, 379-389 (2019).
43. Zhang C, *et al.* Hypoxia induces the breast cancer stem cell phenotype by HIF-dependent and ALKBH5-mediated m(6)A-demethylation of NANOG mRNA. *Proceedings of the National Academy of Sciences of the United States of America* **113**, E2047-2056 (2016).
44. Zhu H, Gan X, Jiang X, Diao S, Wu H, Hu J. ALKBH5 inhibited autophagy of epithelial ovarian cancer through miR-7 and BCL-2. *J Exp Clin Cancer Res* **38**, 163 (2019).
45. Nishizawa Y, *et al.* Oncogene c-Myc promotes epitranscriptome m(6)A reader YTHDF1 expression in colorectal cancer. *Oncotarget* **9**, 7476-7486 (2018).
46. Chen J, *et al.* YTH domain family 2 orchestrates epithelial-mesenchymal transition/proliferation dichotomy in pancreatic cancer cells. *Cell cycle (Georgetown, Tex)* **16**, 2259-2271 (2017).
47. Zhao X, *et al.* Overexpression of YTHDF1 is associated with poor prognosis in patients with hepatocellular carcinoma. *Cancer biomarkers : section A of Disease markers* **21**, 859-868 (2018).
48. Li J, *et al.* Downregulation of N(6)-methyladenosine binding YTHDF2 protein mediated by miR-493-3p suppresses prostate cancer by elevating N(6)-methyladenosine levels. *Oncotarget* **9**, 3752-3764 (2018).
49. Sheng H, *et al.* YTH domain family 2 promotes lung cancer cell growth by facilitating 6-phosphogluconate dehydrogenase mRNA translation. *Carcinogenesis*, (2019).
50. Zhang J, Pi J, Liu Y, Yu J, Feng T. [Knockdown of YTH N(6)-methyladenosine RNA binding protein 2 (YTHDF2) inhibits proliferation and promotes apoptosis in MGC-803 gastric cancer cells]. *Xi bao yu fen zi mian yi xue za zhi = Chinese journal of cellular and molecular immunology* **33**, 1628-1634 (2017).
51. Huang H, *et al.* HNRNPC as a candidate biomarker for chemoresistance in gastric cancer. *Tumour biology : the journal of the International Society for Oncodevelopmental Biology and Medicine* **37**, 3527-3534 (2016).
52. Kleemann M, *et al.* MiR-744-5p inducing cell death by directly targeting HNRNPC and NFIX in ovarian cancer cells. *Sci Rep* **8**, 9020 (2018).
53. Toss A, *et al.* Hereditary ovarian cancer: not only BRCA 1 and 2 genes. *BioMed research international* **2015**, 341723 (2015).

54. Gleicher N, *et al.* Absence of BRCA/FMR1 correlations in women with ovarian cancers. *PLoS One* **9**, e102370 (2014).
55. Drakes ML, Stiff PJ. Understanding dendritic cell immunotherapy in ovarian cancer. *Expert review of anticancer therapy* **16**, 643-652 (2016).
56. Liu R, *et al.* CD47 promotes ovarian cancer progression by inhibiting macrophage phagocytosis. *Oncotarget* **8**, 39021-39032 (2017).
57. Cho U, Kim B, Kim S, Han Y, Song YS. Pro-inflammatory M1 macrophage enhances metastatic potential of ovarian cancer cells through NF-kappaB activation. *Molecular carcinogenesis* **57**, 235-242 (2018).
58. Chen S, *et al.* Neutrophil-to-Lymphocyte Ratio Is a Potential Prognostic Biomarker in Patients with Ovarian Cancer: A Meta-Analysis. *BioMed research international* **2017**, 7943467 (2017).

Supporting Figure Legends

Supporting Figure 1 Relationship between each m6A RNA methylation regulator and age. (A) Heatmap showed that FMR1, METTL16, RBM15 and WTAP have significant association with age. (B) expression levels of FMR1 in high- and low- age groups. (C) expression levels of METTL16 in high- and low- age groups. (D) expression levels of RBM15 in high- and low- age groups. (E) expression levels of WTAP in high- and low- age groups.

Supporting Figure 2 Relationship between each m6A RNA methylation regulator and grade. (A) Heatmap showed that FTO and YTHDC2 have significant association with grades. (B) expression levels of FTO in groups of different grades. (C) expression levels of YTHDC2 in groups of different grades.

Supporting Figure 3 Relationship between each m6A RNA methylation regulator and stage. (A) Heatmap showed that ALKBH5, METTL3, METTL14, METTL16, RBM15 and YTHDF1 have significant association with stage. (B) expression levels of ALKBH5 in groups of different stage. (C) expression levels of METTL3 in groups of different stage. (D) expression levels of METTL14 in groups of different stage. (E) expression levels of METTL16 in groups of different stage. (F) expression levels of RBM15 in groups of different stage. (G) expression levels of YTHDF1 in groups of different stage.

Supporting Figure 4 Relationship between each m6A RNA methylation regulator and tumor-status. (A) Heatmap showed that HNRNPA2B1 and METTL16 have significant association with tumor-status. (B) expression levels of HNRNPA2B1 in groups of different tumor-status. (C) expression levels of METTL16 in groups of different tumor-status.

Supporting Figure 5 Relationship between each m6A RNA methylation regulator and BRCA1 gene mutation. (A) Heatmap showed that FMR1 and YTHDF1 have significant correlation with BRCA1 gene mutation. (B) expression levels of FMR1 in group with BRCA1 mutations and group with no BRCA1

mutation. (C) expression levels of YTHDF1 in group with BRCA1 mutations and group with no BRCA1 mutation.

Supporting Figure 6 OS of the meaningful m6A RNA methylation regulators. (A) ALKBH5, (B) METTL14, (C) METTL16, (D) YTHDF1, (E) YTHDF2, (F) YTHDF3, (G) ZC3H13

Supporting Figure 7 PFS of the meaningful m6A RNA methylation regulators. (A) ALKBH5, (B) METTL14, (C) METTL16, (D) YTHDF1, (E) YTHDF2, (F) YTHDF3, (G) ZC3H13

Supporting Figure 8 ROC curve of the 17 m6A RNA methylation regulators. (A) YTHDC2, METTL3, ZC3H13, WTAP, YTHDF1, YTHDC1, FTO YTHDF2 and ALKBH5 (B) HNRNPA2B1, KIAA1429, FMR1, METTL16, YTHDF3, HNRNPC, RBM15 and METTL14.

Supporting Figure 9 The stratification analysis was performed based on age, grade, tumor status and stage. (A) prognosis of high risk patients was significantly worse than that of low risk patients in the Stage III/IV subgroup. (B) prognosis of high risk patients was significantly worse than that of low risk patients in the grade 3-4 subgroup. (C) high risk patients in subgroup with age ≥ 60 years old were inclined to have unfavorable OS. (D) high risk patients in subgroup with age < 60 years old were inclined to have unfavorable OS. (E) high risk patients in subgroup with tumor were inclined to have unfavorable OS.

Supporting Figure 10 Most significant tumor-infiltrating immune cells and its correlation with immune cell type in OC related to the 3 m6A regulators. (A) Levels of Dendritic fraction in low- and high-risk groups. (B) Levels of Macrophage fraction in low- and high-risk groups. (C) Levels of Neutrophil fraction in low- and high-risk groups.

Supporting Figure 11 Genetic Information of the seventeen Genes. (A) The network constructed by METTL3, HNRNPA2B1, HNRNPC, FMR1 and their 50 most associated neighbor genes. (B) Alternation Frequency of 17 genes. (C) YTHDF1, WTAP and ZC3H13 showed most diverse alteration including amplification, missense mutation etc.

Figures

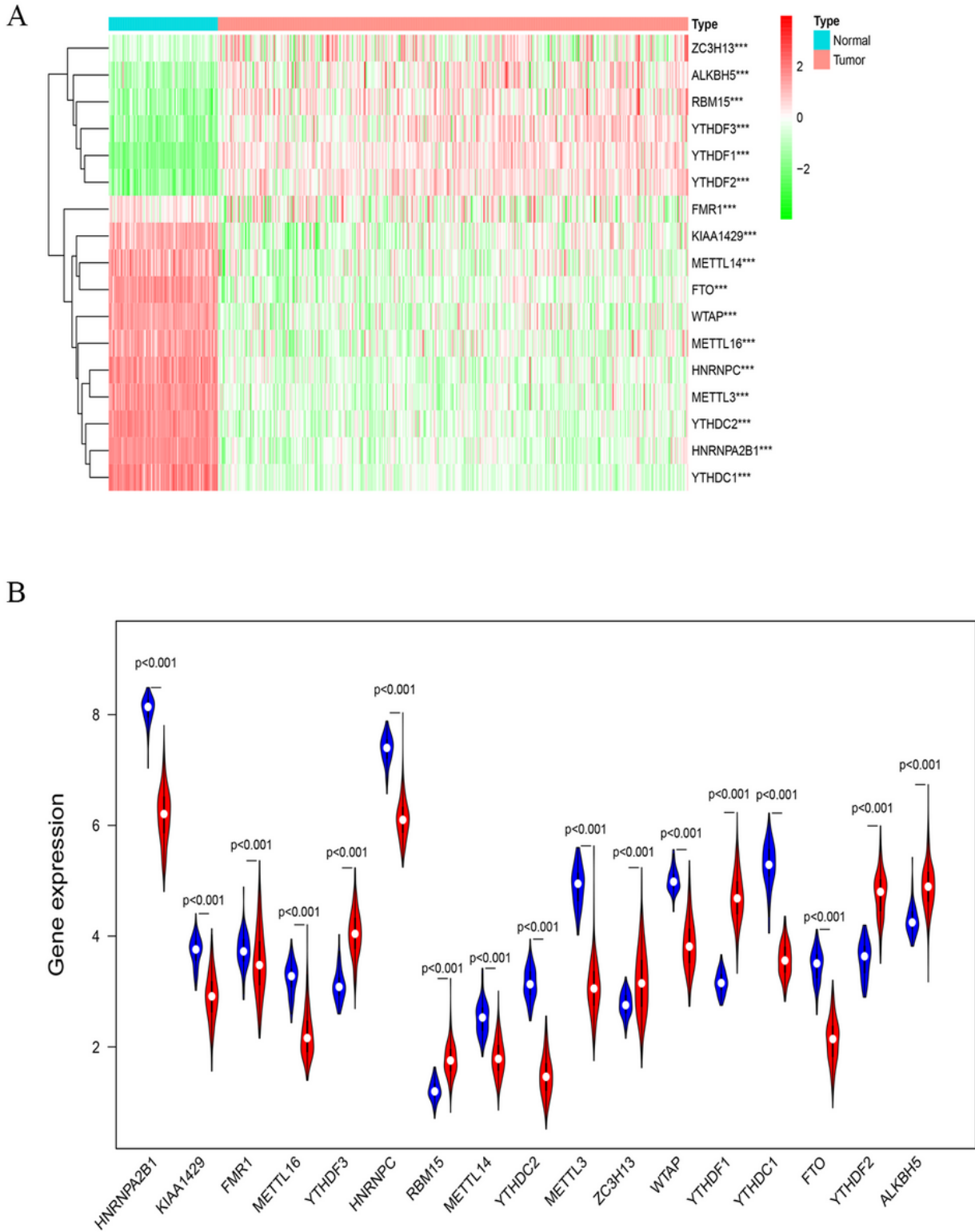


Figure 1

Expression of m6A RNA methylation regulator in OC samples and normal samples. (A) Heatmap showed that the 17 m6A RNA methylation regulators expressed differently between OC samples and normal samples. (B) Expression level of 17 m6A RNA methylation regulators in OC samples and normal samples.

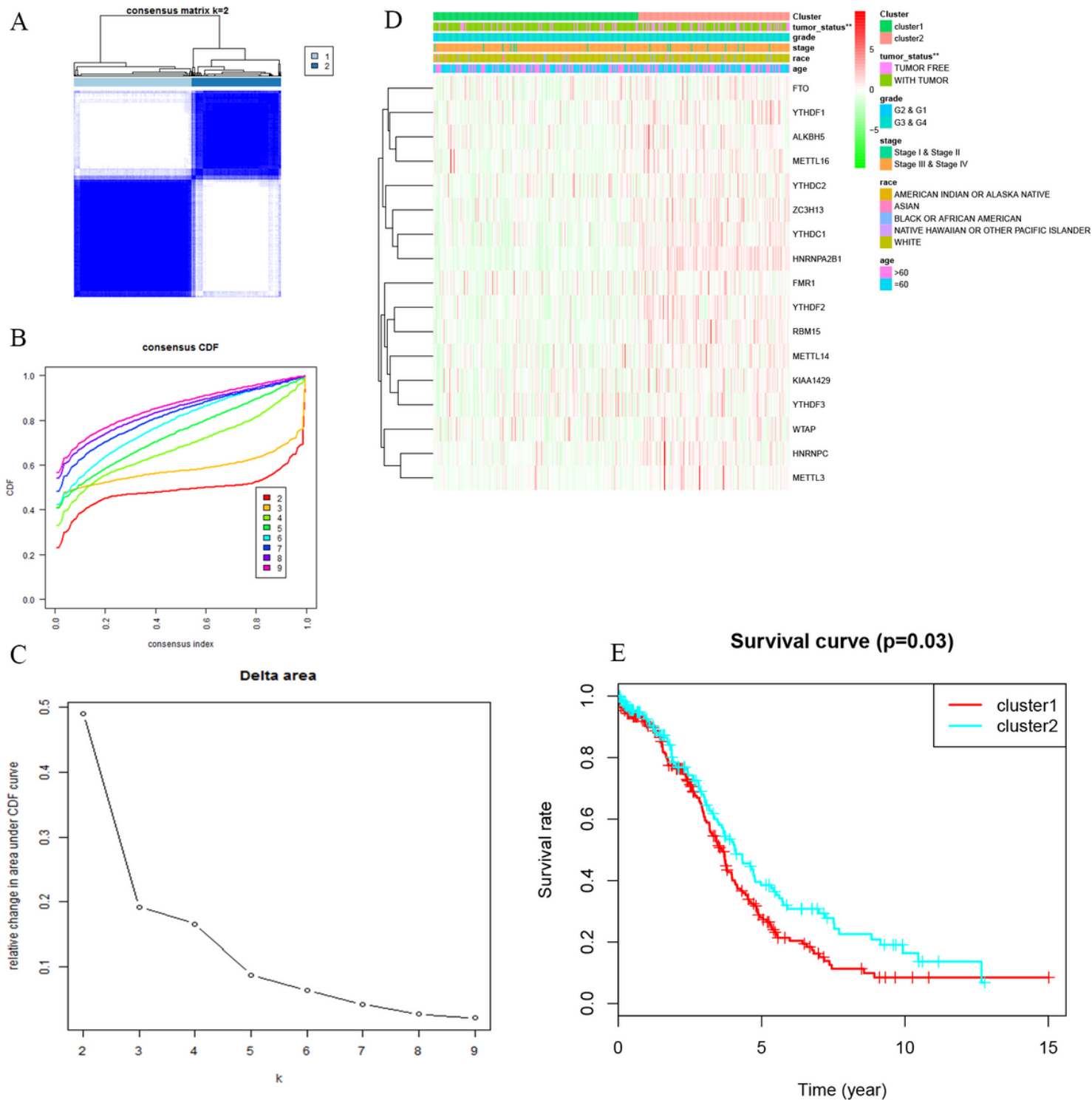


Figure 2

Differential clinicopathological features and overall survival of OC in the cluster 1/2 subgroups. (A) Consensus clustering matrix of 379 TCGA samples for k = 2. (B) Consensus clustering cumulative distribution function (CDF) for k = 2 to 10. (C) Relative change in area under CDF curve for k = 2 to 10. (D) Heatmap and clinicopathologic features of the two clusters defined by the m6A RNA methylation regulators consensus expression. (E) Kaplan–Meier overall survival (OS) curves for 315 out of 379 OC samples in the TCGA dataset.

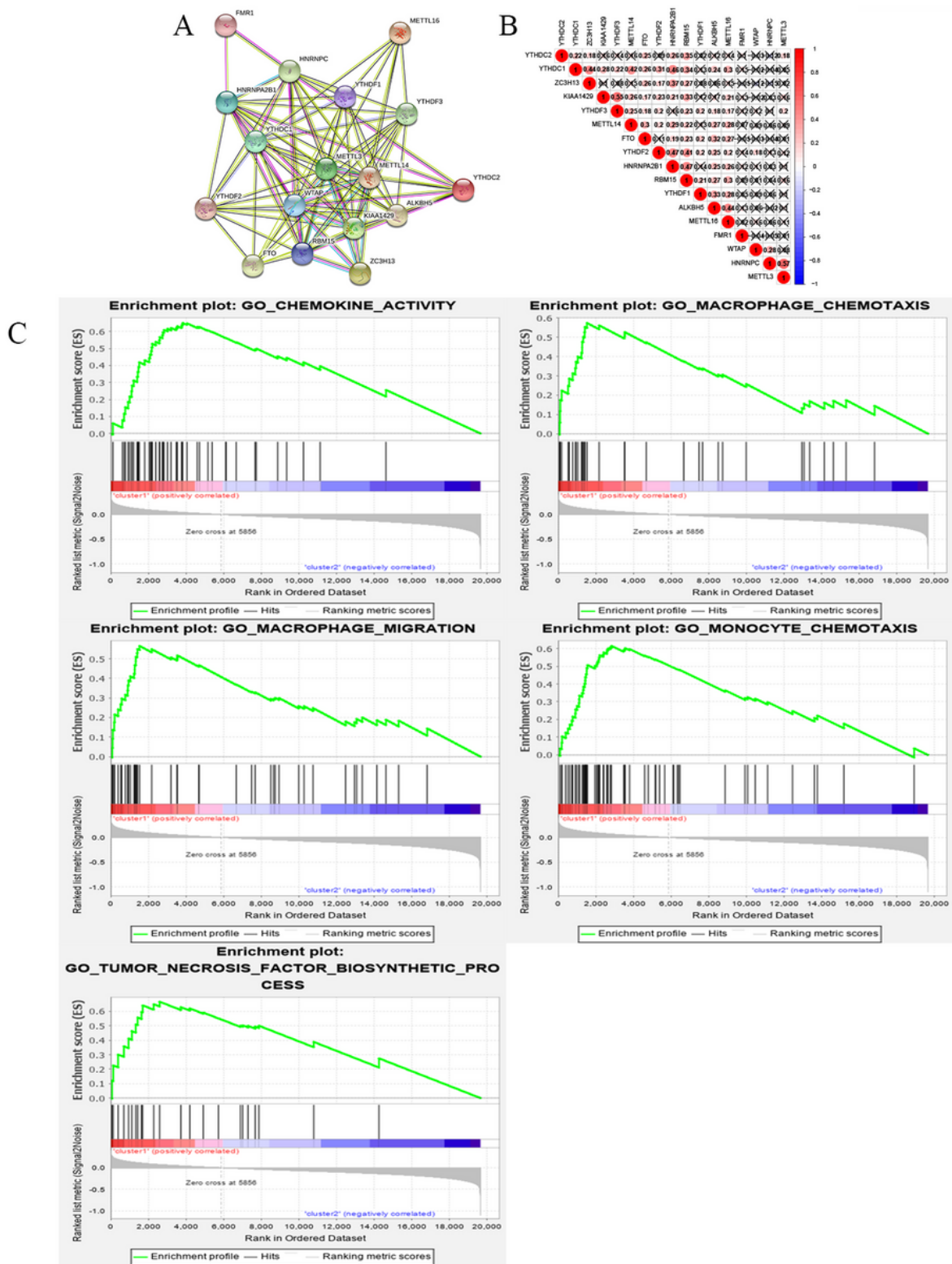


Figure 3

Interaction among m6A RNA methylation regulators and functional annotation of OC in cluster 1/2 subgroups. (A) The m6A modification-related interactions among the 17 m6A RNA methylation regulators. (B) Spearman correlation analysis of the 17 m6A modification regulators. (C) GO analysis by GSEA of cluster1 and cluster 2.

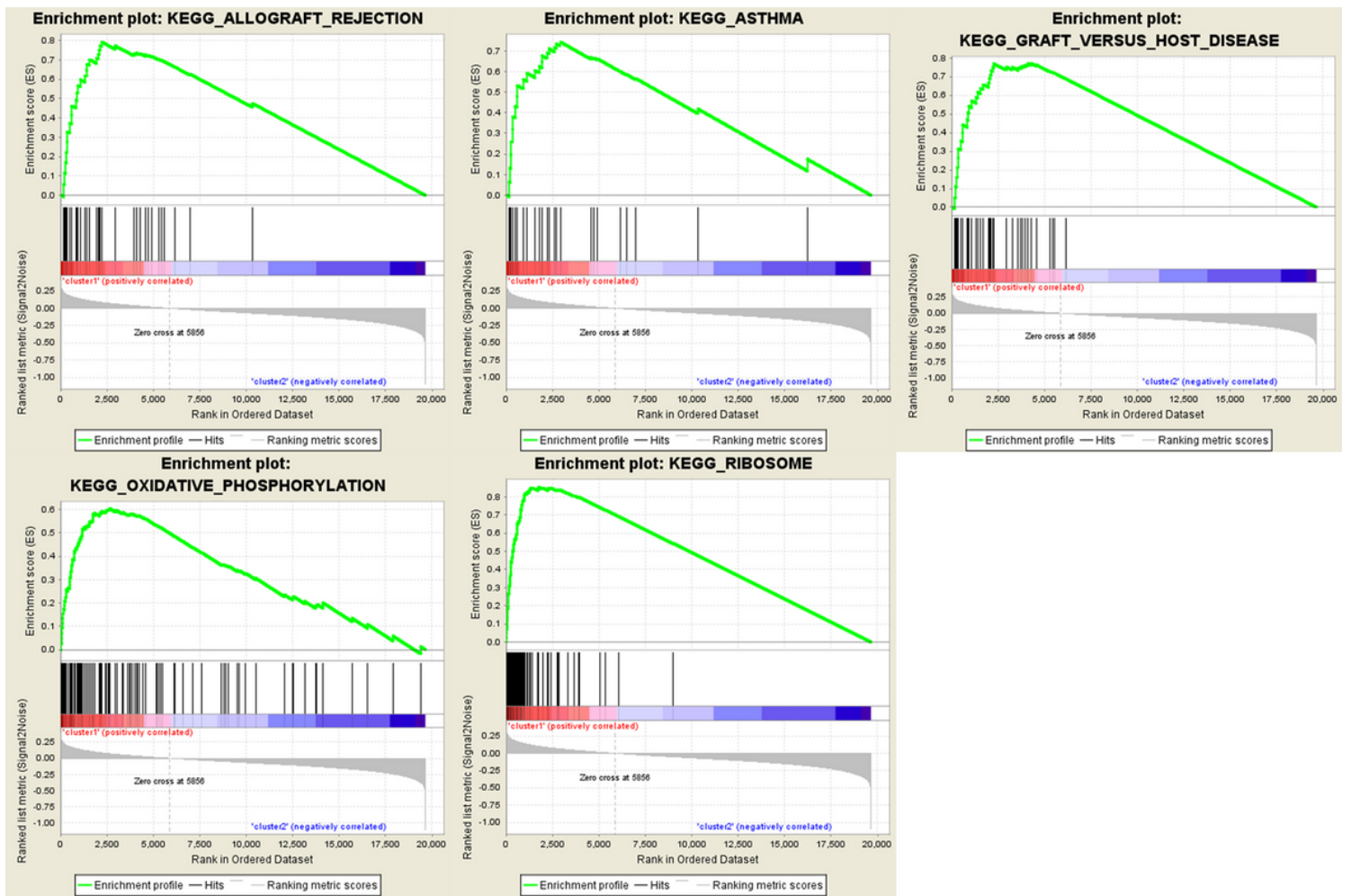


Figure 4

Gene set enrichment analysis was functioned to show the most relative pathway.

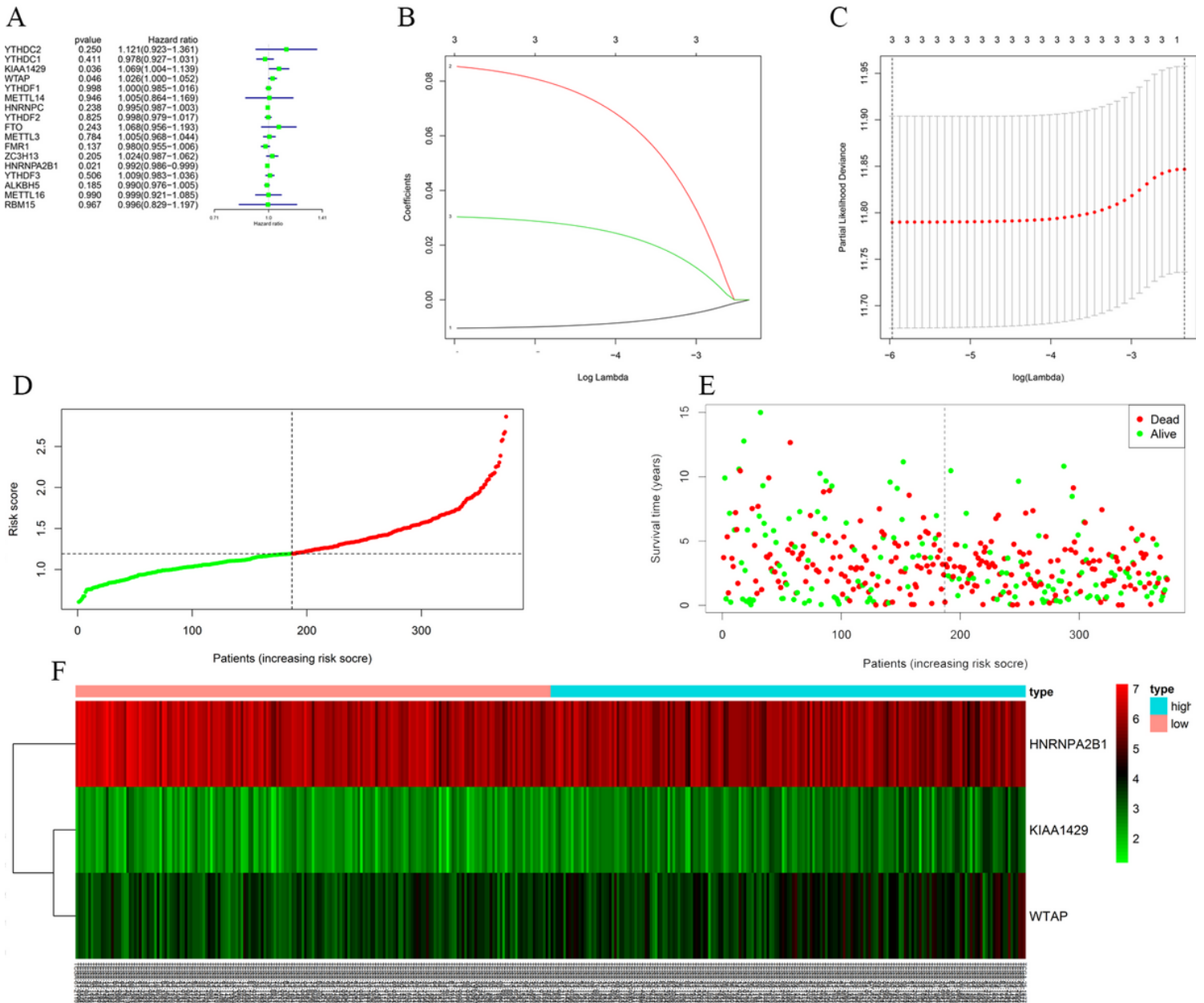


Figure 5

Risk signature with 17 m6A RNA methylation regulators. (A) The process of building the signature containing 17 m6A RNA methylation regulators. The hazard ratios (HR), 95% confidence intervals (CI) calculated by univariate Cox regression. (B-C) the coefficients calculated by LASSO. (D-E) The risk scores for all patients in TCGA cohort are plotted in ascending order and marked as low risk (blue) or high risk (red), as divided by the threshold (vertical black line). (F) The distribution of risk score, survival status, and the expression of 3 genes of each patient in TCGA cohort by z-score, with red indicating higher expression and light blue indicating lower expression.

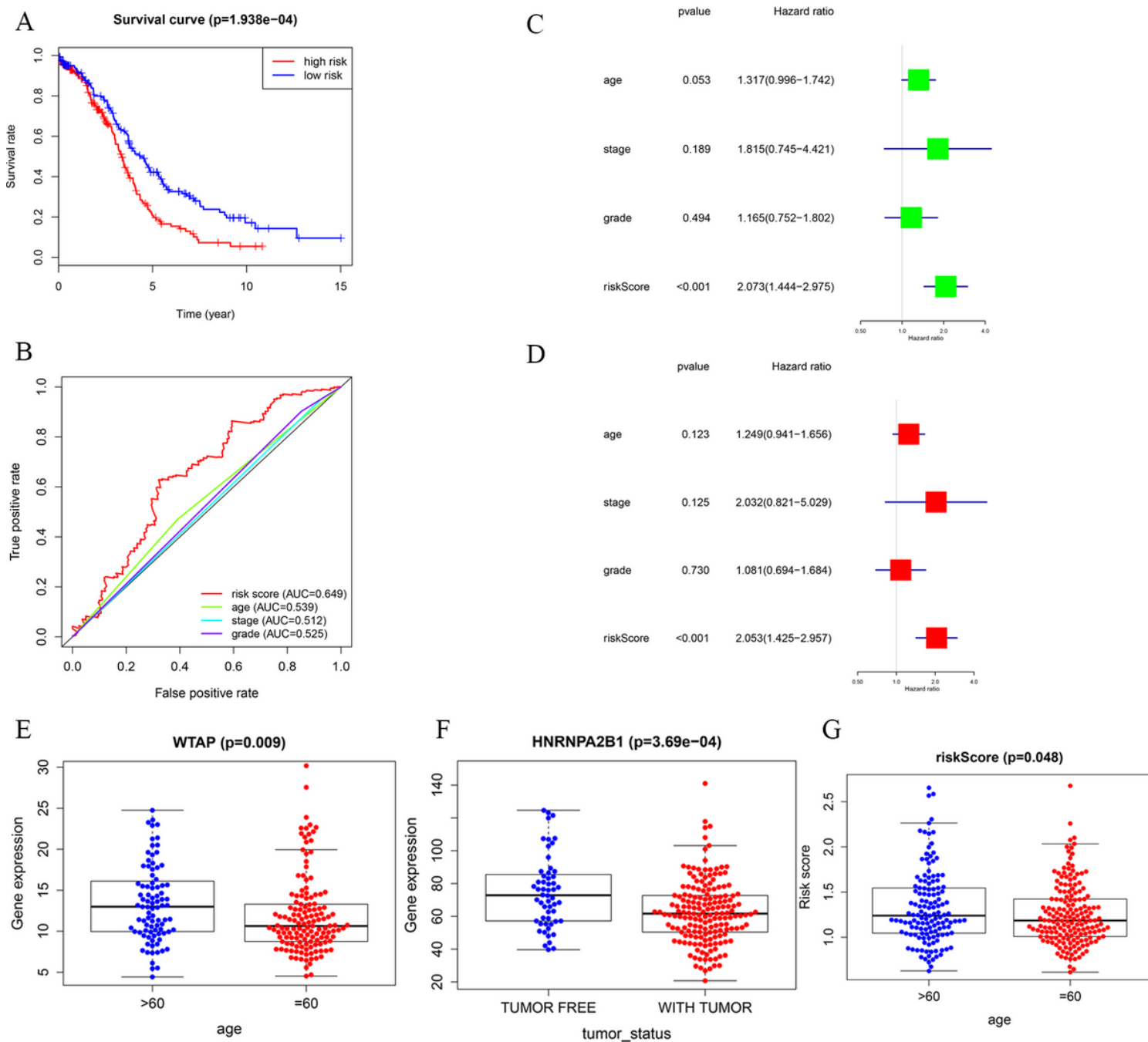


Figure 6

Screening of Prognosis-related m6A RNA methylation regulators. (A) OS between the low- and high-risk groups. (B) ROC curve analysis. (C) univariate regression model. (D) multivariate regression model. (E) WTAP expression levels in different age groups. (F) The expression levels of HNRNPA2B1 in the TUMOR FREE group and the TUMOR group. (G) RISK SCORE in different age groups.

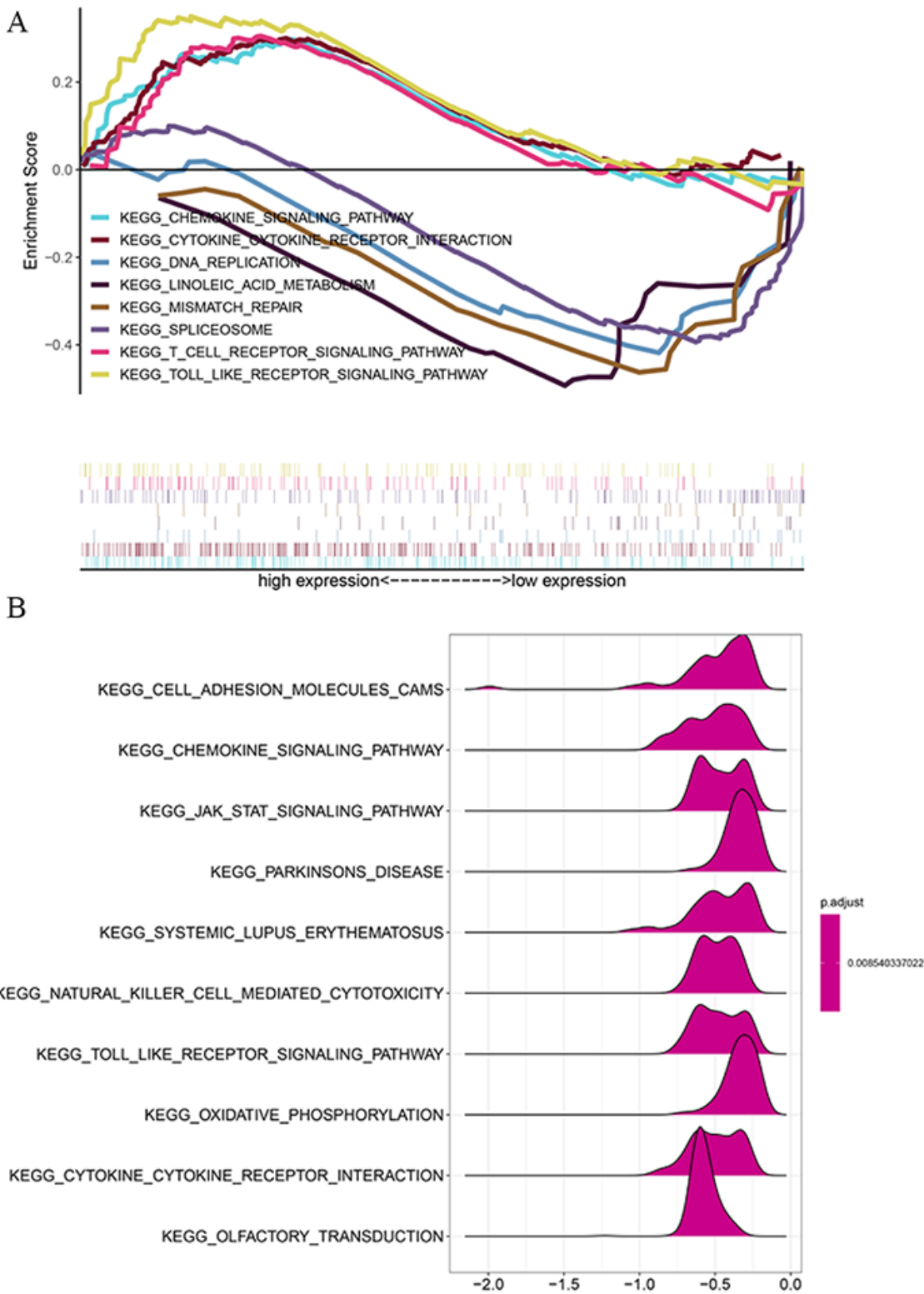


Figure 7

GSEA results and KEGG enrichment. (A) GSEA plots of 'KEGG-pathways' enriched in high- and low-risk OC patients in TCGA dataset. (B) GSEA plots of KEGG Pathways in which the WTAP, KIAA1429 and HNRNPA2B1 were co-enriched.

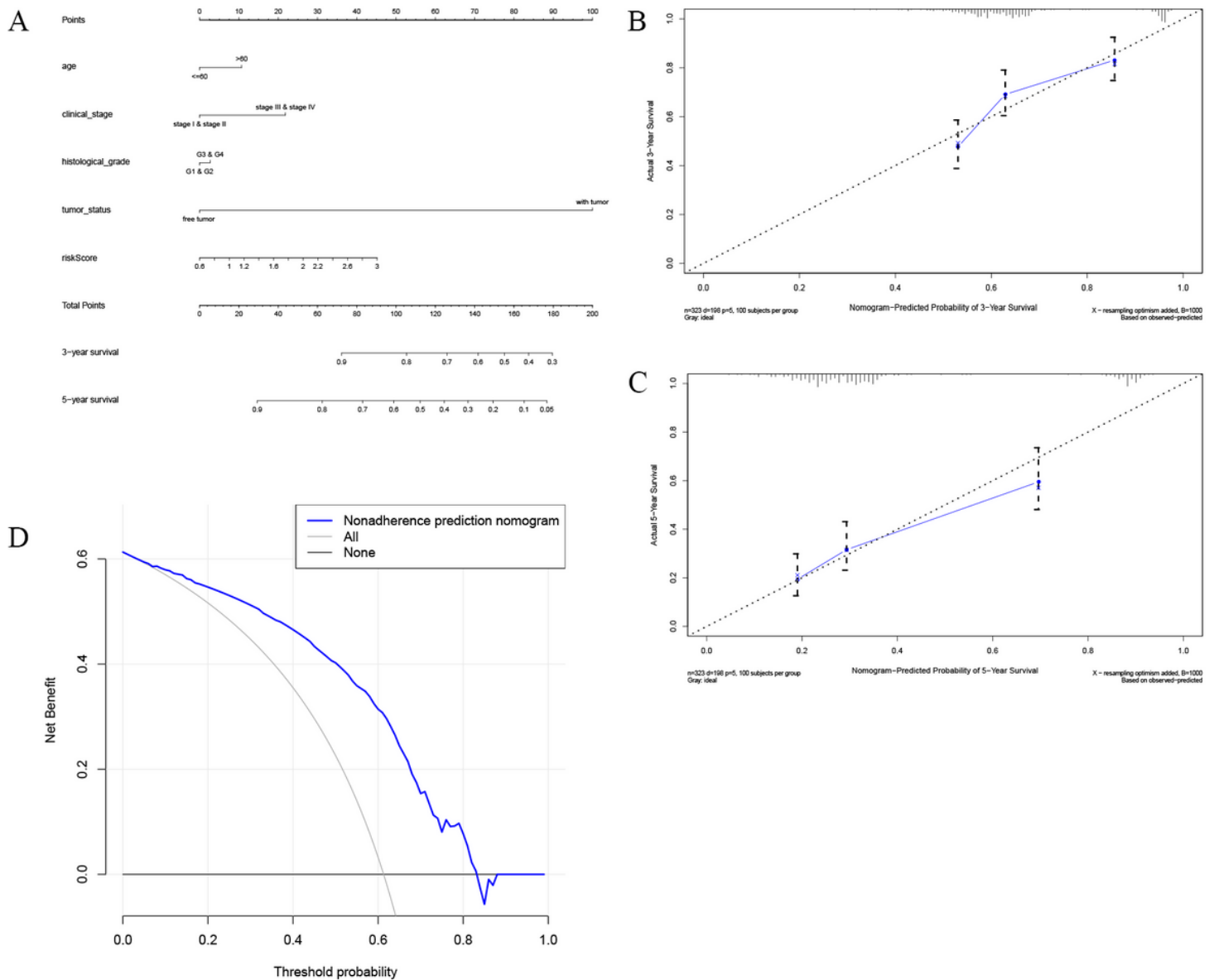


Figure 8

The nomogram to predict 3- or 5-year OS in the entire set. (A) The nomogram for predicting proportion of patients with 3- or 5-year OS. (B-C) The calibration plots for predicting patient 3- or 5-year OS. Nomogram-predicted probability of survival is plotted on the x-axis; actual survival is plotted on the y-axis. (D) DCA for assessment of the clinical utility of the nomogram. The x-axis represents the percentage of threshold probability, and the y-axis represents the net benefit. DCA: decision curve analysis; OS: overall survival.

Supplementary Files

This is a list of supplementary files associated with this preprint. Click to download.

- [SupportingFigure10.tif](#)

- SupportingFigure11.tif
- SupportingFigure1.tif
- SupportingFigure3.tif
- SupportingFigure4.tif
- SupportingFigure7.tif
- SupportingFigure2.tif
- SupportingFigure9.tif
- SupportingFigure6.tif
- SupportingFigure8.tif
- SupportingFigure5.tif